Hindawi
Wireless Communications and Mobile Computing
Volume 2022, Article ID 4213217, 9 pages
https://doi.org/10.1155/2022/4213217

Research Article

Artificial Intelligence of Things-Based Optimal Finite-Time Terminal Attractor and Its Application to Maximum Power Point Tracking of Photovoltaic Arrays in Smart Cities

En-Chih Chang, Chun-An Cheng, and Rong-Ching Wu

Department of Electrical Engineering, I-Shou University, No. 1, Sec. 1, Syuecheng Rd., Dashu District, Kaohsiung City 84001, Taiwan

Correspondence should be addressed to En-Chih Chang; enchihchang@isu.edu.tw

Received 6 January 2022; Revised 5 March 2022; Accepted 17 March 2022; Published 7 April 2022

Academic Editor: Chao-Yang Lee

The combination of artificial intelligence of things (AIoT) and photovoltaic power generation can save energy and reduce carbon emissions and further promote the development of smart cities. In order to obtain the maximum power output from photovoltaic (PV) arrays, we can use optimal maximum power point tracking (MPPT) technique with AIoT sensing to improve system efficiency. The optimal MPPT technique is the finite-time terminal attractor (FTTA) based on the gradient particle swarm optimization (GPSO), which can be applied to track the maximum power of a PV array system. The FTTA not only provides fast finite-time convergence but also attenuates steady-state errors, making it ideal for nonlinear system applications. The GPSO is used to search the control parameters of the FTTA, which is able to find the global best solution. This avoids unmodeled dynamic behavior of the system excited by the quiver, which slows down the control convergence and prematurely traps the system into a local optimum. The MATLAB computer software is used to simulate the proposed PV maximum power point tracking system. The results show that more accurate and better tracking control of the PV array can be produced under partial shading conditions and then improve the steady-state and transient performance.

1. Introduction

With advances in technology, solar energy is becoming the most cost-effective long-term investment [1–3]. Like any equipment, solar systems must be managed effectively to optimize energy and power production. With solar smart cloud monitoring, users can get real-time information on PV power generation through the Internet and collect environmental information from the site to ensure the efficiency of the PV array system. Therefore, how to maximize the performance of solar cells has been one of the most important development projects in various countries around the world and is also the most important issue in solar energy-related technology. With the aim of attaining PV array systems with maximum power tracking, a DC-DC power converter including maximum power tracking control method modulates the solar cell output to deliver maximum power [4–7]. There are many research works presenting all kinds of maximum power point tracking (MPPT) alternatives, such as incremental conductivity, perturbation observation, most valuable player methodology, and fuzzy logic [8–11]. There are couplings among sunlight brightness as well as atmospheric climate and the changes in PV maximum output power. The majority of the MPPT algorithms fails to perform a rigorous evaluation of both convergence and reliability and even cannot preserve stable pursuit of the maximum power point quickly. The sliding mode control (SMC) has simplified architecture, allows effortless design, and gives the system robustness against changes in internal parameters as well as external perturbations [12–18]. There are lots of useful SMC publications for controlling PV array systems [19–22]. However, photovoltaic array systems controlled by the SMC are subject to uncertainties. The state convergence time of such a system is not limited and quiver arises, thus compromising system performance in the steady-state

and transience. The quivering can be particularly problematic in practice, as it not only implies excessive energy consumption but also can provoke unmodeled high-frequency plant dynamics. There have been suggested solutions to ameliorate the quiver problem, such as estimator and adaptive methods. Even though they have improved the quiver problem and also enhanced the transience behavior of the system in the presence of unspecified disturbances, the mathematically complex and computationally time-consuming exist [23–25]. With explicit convergence and stability analysis, the finite-time terminal attractor (FTTA) not only provides the design approach for the robustness of the conventional sliding law, but more specifically, it provides a finite system state convergence time, i.e., a finite time for the system trajectory to reach the sliding mode zone in the presence of uncertainties. This methodology further strengthens the dynamical characteristics of the system and minimizes steady-state errors as well as quiver problems [26–29]. However, what is more important to note is that even though the FTTA allows the PV system to achieve the desired control effect, PV arrays may be partially shaded by buildings, wood, pollution, etc., degrading power output and leading to energy loss. There will be no regular fluctuation in the PV output power which resides in multiple local extremes. If the conventional MPPT methods described previously (e.g., disturbance observation, incremental conductivity, most valuable player methodology, and fuzzy logic) are used, they will be traced to the local extremes (local maximum power points) rather than the global extremes (global maximum power points). There have been several approaches tried to tackle multiple local extrema, such as the grey wolf optimizer and the brute force algorithm [30–32]. The grey wolf optimizer is fast, but it is constrained to local searching and incapable of searching globally. The brute force algorithm gives a superior ability to seek the best solution, but it has the weakness in needing a longer seeking time which stagnates easily on a certain solution. The gradient particle swarm optimization (GPSO) algorithm is based on the concept of gradient mechanism, showing simplified computation and enhanced population diversity that can demonstrate global domain search capability and has been widely used to solve many optimization problems [33–37]. It can improve the drawback of traditional PSO algorithm which tends to prematurely converge into local extrema [38–42]. The GPSO is therefore used to calculate the voltage reference value of the maximum power point of the PV array in the event of partial shading. In this paper, a GPSO is used to find the global extrema of the PV array under partial shading, and then, a FTTA is employed for its tracking control, providing good control power output to maintain the highest conversion efficiency of the PV array system. As a result, the FTTA based on the GPSO will improve the quiver problem, lessen the steady-state error, shorten the system state convergence time, solve the multipeak phenomenon (local maximum power point), and then render the PV MPPT system to have good steady state and dynamic response at the same time. The proposed controller with simplicity and high speed convergence as well as easy programming permits higher accuracy and stable following control. Computer simulations display that the proposed controller will provide the PV MPPT system to improve steady-state performance and transient tracking speed in the presence of partial shading or under highly uncertainty conditions. The proposed system is also compared with a conservative sliding mode controlled PV MPPT system to show the superior performance and theoretical applicability of the proposed system.

2. Modeling of PV MPPT System

A solar energy system usually consists of a PV array, a DC-DC converter, a DC-AC inverter, and the attached load. With changes in brightness as well as temperature, there will be a reference value for the voltage corresponding to the maximum power point of the PV system. Therefore, an interleaved Boost DC–DC converter (Figure 1) is used to adjust the PV array voltage (for the maximum power point voltage). The dynamic equation of the interleaved Boost DC–DC converter is derived from the state-space averaging method for the PV system as follows:

$$\begin{cases} \dot{i}_{db} = -2L_{dbL}^{-1}[v_{dbo} \cdot (1-u) - i_{db} \cdot R_{dbL} - v_{dbi}], \\ \dot{v}_{dbo} = C_{db}^{-1}\left[i_{db} \cdot (1-u) - v_{dbo} \cdot {R_{db}}^{-1}\right], \end{cases} \tag{1}$$

where $i_{db} = i_{db1} + i_{db2}$, v_{dbi} is the PV array output voltage, i_{dbo} indicates the PV array output current, i_{dbo} denotes the output load current, v_{dbo} means DC output voltage, u symbols control input, $L_{dbL} = L_{dbL1} = L_{dbL2}$ and $R_{dbL} = R_{dbL1} = L_{dbL2}$, here R_{dbL1} and R_{dbL2} refer to the equivalent series resistance of inductors L_{db1} and L_{db2}, respectively. Let v_{dem} be the voltage reference of the maximum power point calculated by the GPSO algorithm, and in order to make v_{dbo} follow v_{dem}, the FTTA closed-loop control technology is necessary to achieve such a result. In other words, in a PV system, the error in the output voltage can be defined as the state variable $\tilde{x}_2 = v_{dbo} - v_{dem}$, which is regulated from the state variable $\tilde{x}_1 = i_{db}$ feed current. Our goal is to design the control law u properly. If it is well designed, (1) will be stable and the error $\tilde{x}_2$ quickly converges to the balance point. The PV output voltage will be the same as the required reference voltage. Even if the PV MPPT system is partially shaded or malfunctioning or under nonmatching uncertainty, the tracking control can still be fast, accurate, and robust.

Then, a single-phase PWM DC–AC inverter is used to convert the generated DC power into AC power for transmission to the grid. A typical single-phase PWM inverter is shown in Figure 2, where four semiconductor switches, LC filters, and loading (resistive loading or capacitive input rectifier loading) are considered as the plant to be handled. Owing to the diversity of the loading connected to the inverter, it is not possible to develop a general model that is representative of every type of load. In this case, a nominal load is defined to derive a linear model, where load changes and model uncertainties are regarded as disturbances. Furthermore, in view of the assumption that the switching frequency is much higher than the modulation frequency of the inverter, the dynamics of the single-phase PWM DC–AC inverter is mainly handled by its LC filter and the attached load, which can be modeled as a second-order linear system. Based on Kirchhoff's voltage and current laws, the state equations of the inverter can be described as follows:

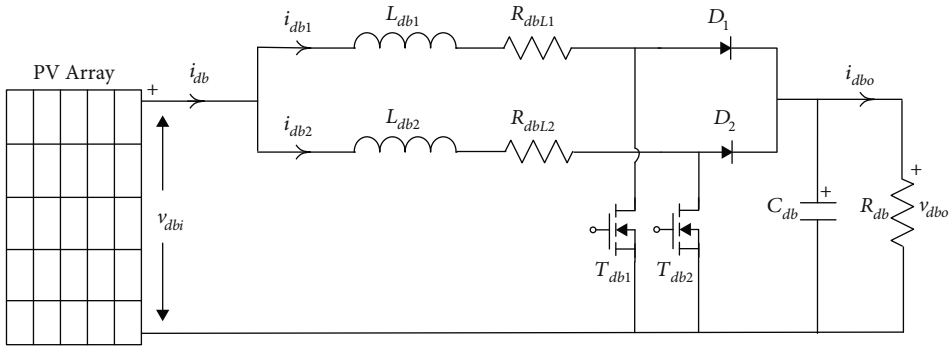

Figure 1: Interleaved Boost DC–DC converter.

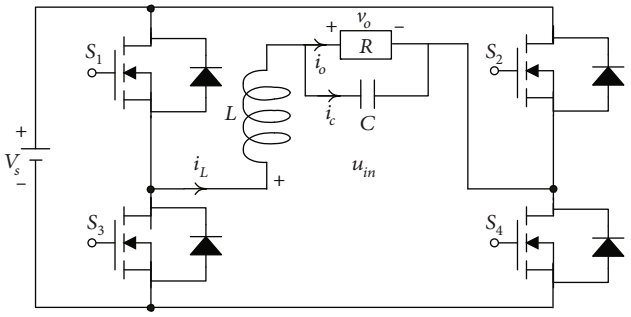

Figure 2: Single-phase PWM DC–AC inverter.

$$L\dot{i}_L + v_o = u_{\text{in}}, \tag{2}$$

$$i_L = C\dot{v}_o + \frac{v_o}{R}, \tag{3}$$

where u_{in} is equal to $V_s \cdot d$ (time-averaging technique), where d indicates the duty ratio of switching ranging from negative one to positive one and V_s represents the DC link voltage.

The differential equation is obtained by replacing (3) in (2) in the following.

$$\ddot{v}_o + \frac{1}{\text{RC}}\dot{v}_o + \frac{1}{\text{LC}}v_o = \frac{1}{\text{LC}}u_{\text{in}}. \tag{4}$$

The state variables are specified $x_1 = v_o$ and $x_2 = \dot{v}_o$, whereupon (4) can be formulated as the result of the state-space form below:

$$\begin{bmatrix}\dot{x}_1\\ \dot{x}_2\end{bmatrix} = \begin{bmatrix}0 & 1\\ -\dfrac{1}{\text{LC}} & -\dfrac{1}{\text{RC}}\end{bmatrix}\begin{bmatrix}x_1\\ x_2\end{bmatrix} + \begin{bmatrix}0\\ \dfrac{1}{\text{LC}}\end{bmatrix}u_{\text{in}}. \tag{5}$$

The design problem of the inverter is equivalent to a typical tracking control issue since the output voltage of the inverter is a sinusoidal waveform. Allow v_{ref} to be the desired sinusoidal waveform that v_o will have to follow. Through the definition of the error state variables $e_1 = x_1 - v_{\text{ref}}$ and $e_2 = \dot{x}_1 - \dot{v}_{\text{ref}}$, it is possible to acquire the tracking control error state equation as follows:

$$\begin{bmatrix}\dot{e}_1\\ \dot{e}_2\end{bmatrix} = \begin{bmatrix}0 & 1\\ -a_1 & -a_2\end{bmatrix}\begin{bmatrix}e_1\\ e_2\end{bmatrix} + \begin{bmatrix}0\\ b\end{bmatrix}u_{\text{in}} + \begin{bmatrix}0\\ 1\end{bmatrix}w, \tag{6}$$

where $a_1 = 1/\text{LC}$, $a_2 = 1/\text{RC}$, and $b = 1/\text{LC}$ and $w = -a_1 v_{\text{ref}} - a_2\dot{v}_{\text{ref}} - \ddot{v}_{\text{ref}}$ denotes the disturbance, with the variable e_1 being a difference measurement between v_o and v_{ref}. The system (6) will become stable where e_1 eventually converges to zero with the control signal u_{in} being completely designed so that the output of the inverter is kept at the same level as the desired v_{ref}. In order to allow the error states converged to zero, the control law u_{in} can be designed via discrete proportional–integral-differential scheme. The significance of the inverter in the system needs to be specifically pointed out as follows. The inverter is the key equipment of a PV generation system, mainly serving as the interface between the PV arrays as well as the power grid. The absence of an inverter will not create a completely operational and autonomous PV generation system for residential or commercial use. In this system configuration, there are two power-converting stages. The DC-DC converter handles maximum power point tracking (MPPT) as well as adjusts the DC loading voltage. While the grid-connection occurs, the power is produced by PV arrays which are converted by the DC-AC inverter into high-quality AC output. Also, it is worth observing that the sampling rate (1/sampling time) acts as a significant deciding point for the performance of the control. It is advisable to adopt a high sampling rate (which leads to a less total harmonic distortion, even at rectified loads) in order to achieve a superior level of control. It implies the possibility of using a digital control system with the maximum frequency, alternatively an analogue design reflecting the algorithm of control [43–45].

3. Control Design

The problem statement for nonlinear systems using the classical TA is briefly summarized, and then, an improved technique is designed. Consider the following classical TA sliding surface as

$$\Lambda = \dot{x}_1 + \eta x_1^{m_1/m_2}, \tag{7}$$

where x_1 is the system variable, η signifies positive constant,

and $0 < m_1/m_2 < 1$. An SMC law $u = u_{\text{upper}}(x)$, $u_{\text{lower}}(x)$ can be used, representing $\Lambda > 0$, $\Lambda < 0$, which is expressed as driven Λ to the sliding mode $\Lambda = 0$ during finite time. As such, it is possible to control the dynamics of the system as

$$\Lambda = 0 = \dot{x}_1 + \eta x_1^{m_1/m_2}. \tag{8}$$

There is a finite time T_f for getting from the starting state $x_1(0)$ to zero that arises from the following:

$$T_f = \eta^{-1} \frac{|x_1(0)|^{1-m_1/m_2}}{(1 - m_1/m_2)}. \tag{9}$$

In this case, it is revealed that the system state is converged to zero for a finite time duration. Taking into account the Jacobian matrix $= \partial \dot{x}_1/\partial x_1$, there is a convergence of the system states to zero around the balancing point $x_1 = 0$ at finite time. The eigenvalues of the Jacobian matrix are derived to be negatively infinite, as x_1 tends to zero. As the speed of the system trajectory towards the balancing point becomes infinite, this causes time reachability to be limited. Yet, the equivalent control section suffers from the issues listed below. In the case of $\dot{x}_1 \neq 0$, as well as $x_1 = 0$ and $0 < m_1/m_2 < 1$, the control law probably gives rise to a singularity. An unknown control signal is generated by this singularity, which induces an unstable feedback system. (ii) For the condition $0 < m_1/m_2 < 1$, it is possible to have an imaginary number $x_1^{m_1/m_2 - 1}$.

Therefore, the FTTA is proposed to improve the conservative TA, and its sliding function based on the system dynamics (1) is represented as

$$\Lambda = \tilde{x}_2 + \rho_1^{-1} \|\tilde{x}_2\|^{\kappa+1} + \rho_2^{-1} \dot{\tilde{x}}_2^{m}, \tag{10}$$

where $\kappa_1 > 0$, $\rho_1 > 0$, $\rho_2 > 0$, and $1 < m < 2$. Simultaneously, it is recommended that the sliding mode reaching law, i.e.,

$$\dot{\Lambda} = -\sigma_1 \Lambda - \sigma_2 |\Lambda|^k \text{sigm}(\Lambda), \tag{11}$$

where $\sigma_1 > 0$, $\sigma_2 > 0$, $0 < k < 1$, and $\text{sigm}(\Lambda) = [2/(1 + e^{-\Lambda/\varepsilon})] - 1$ is a smooth sigmoidal function with a positive constant ε.

Recapitulating (1), the dynamics can be written as $\dot{\tilde{x}} = p(\tilde{x}(t)) + q(\tilde{x}(t))u$; here, p and q denote the functions. Then, it is possible to derive the control law of FTTA to be

$$u = -q^{-1}\left[K_e \tilde{x} + \rho_2 m^{-1} \dot{\tilde{x}}_2^{2-m} \frac{(1 + (\kappa+1)\|\tilde{x}_2\|^{\kappa})}{\rho_1}\right] - q^{-1}\left[\sigma_1 \Lambda + \sigma_2 |\Lambda|^k \text{sigm}(\Lambda)\right], \tag{12}$$

where K_e represents the feedback gain of equivalent control, which creates the desired sliding mode while system uncertainties equal to zero. Equation (12) leads to the system state will be compelled towards $\Lambda = 0$, which converges in a finite amount of time.

$$\nu_{j+1} = W\nu_n + \ell_1 \text{RAN}_1\left(\chi_{pb,j} - \chi_j\right) + \ell_2 \text{RAN}_2\left(\chi_{gb,j} - \chi_j\right), \tag{13}$$

$$\chi_{j+1} = \chi_j + \nu_{j+1}, \tag{14}$$

where ν_{j+1} represents present flying speed, χ_j indicates present position, χ_{pb} shows individual best position, χ_{gb} stands for global best position, ℓ_1 and ℓ_2 signify learning factor, RAN_1 and RAN_2 are random number amidst zero and one, and W denote inertia weight. Then, let the function $G(\chi)$ advance in the direction of its fastest descent, namely, the direction of the negative gradient $-\nabla G(\chi)$. It will gradually move towards the optimum so that the negative gradient arises from the condition of $(j-1)$ generation to j generation as follows:

$$-\nabla G(\chi) = \frac{\left[G\left(\chi_{j-1}\right) - G\left(\chi_j\right)\right]}{\nu_j}, \tag{15}$$

where the symbol ∇ stands for gradient operator. One may choose carefully, W is positive in case $G(\chi_{j-1})$ is greater than equal to $G(\chi_j)$; otherwise, W is negative. The proposed algorithm converges fast as well as the searching of the gradient at the global best position. Because there is a constant or minor variation in its fitness value depending on a prescribed iteration number, the computational burden of the proposed algorithm diminishes [46–48]. It is important to note that the voltage, current, and power of the PV array vary with the strength of daylight as well as climate, which impacts both the power output and energy efficiency of the system. As the environmental temperature rises, there will be a reduction in the maximum power of the PV array. However, increasing irradiation levels result in potentially greater maximum PV power. To allow the PV array system to be more efficient, a MPPT function becomes imperative. Once the solar cell module approaches the maximum power point, the derivative of power with respect to voltage becomes zero. Thus, one always operates the PV array at the maximum power point through power converters together with the MPPT algorithm. More precisely, the design of the MPPT controller can be summarized as follows. (i) The overall number of particles and particle locations as well as velocities are initialized and the fitness values can be estimated. (ii) Determine each particle voltage relative to the PV array output power, as well as initialize the group best voltage. (iii) Renew the particles and execute the gradient search in accordance with (13)–(15). (iv) Allow the voltage of all particles in the group to be renewed for one-round iteration g; afterwards, the g-th particle voltage should be renewed as well as estimate the output power of the PV array working at such a voltage. (v) Update the best voltages of the particles themselves and the group. (vi) Check whether the convergence criterion has been fulfilled. In case of yes, the best solution can be obtained; otherwise, step (iii) is continued.

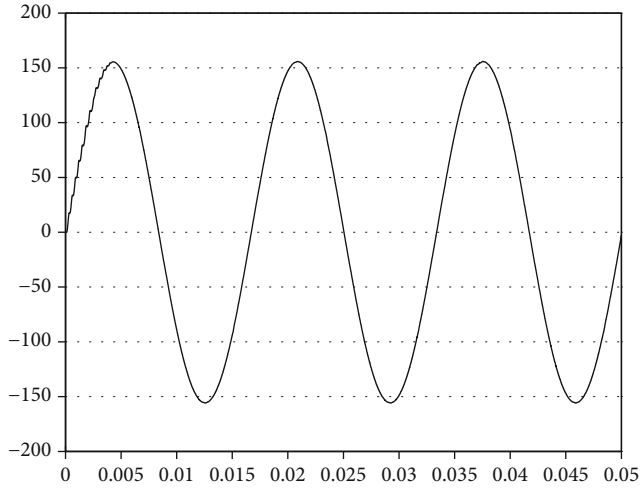

Figure 3: Output voltage of a PV array system for the conservative SMC under resistive load (vertical: 50 V/div; horizontal: 5 ms/div).

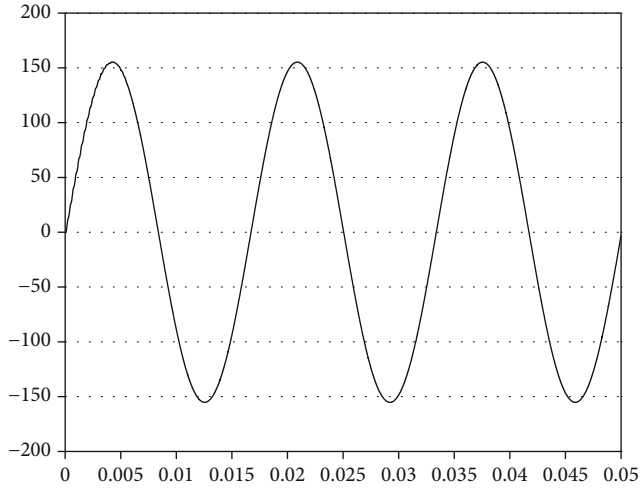

Figure 4: Output voltage of a PV array system for the proposed controller under resistive load (vertical: 50 V/div; horizontal: 5 ms/div).

Proof. The definition of a Lyapunov candidate gives the following $V = \Lambda^2/2$, and based on the dynamical system trajectory along from the control law (10) with the use of the Lyapunov candidate, time derivative of V becomes $\dot{V} = \Lambda\dot{\Lambda} = \Lambda(\tilde{x}_2 + \rho_1^{-1}\|\tilde{x}_2\|^{\kappa+1} + \rho_2^{-1}\dot{\tilde{x}}_2^m)'$. Because m is fractional satisfying $1 < m < 2$, and when $\dot{\tilde{x}}_2 \neq 0$, $\dot{\tilde{x}}_2^{m-1} > 0$ is valid. For $\rho_2 > 0$, therefore $\dot{V} \leq 0$ holds. Under the condition $\dot{\tilde{x}}_2 \neq 0$, it is proven that the system fulfills the Lyapunov stability condition which allows it to quickly arrive at the sliding surface within a finite time. Yet, there is quiver or steady-state error in the FTTA. This is caused by drastic variations or great nonlinearities in the system load, which prevent the eventual system output from following the reference sine wave, rendering the tracking behavior imprecise. Aiming to acquire the global best solution, the GPSO algorithm can be used. Equations (13) and (14) represent the model of particle evolution, which can then update the velocity and location of each particle as it flies to its target. □

4. Results and Discussion

In order to verify the effectiveness of the proposed controller, the system is tested under steady-state response for full resistive loads and rectifier loads and transient response for step load changing. Figure 3 shows the output voltage (%THD = 0.05%) of the PV array system with a resistive load $R = 12\,\Omega$ for the conservative SMC. It can be seen that the output voltage is very close to a sine wave. Figure 4 shows the output voltage (%THD = 0.02%) of the proposed controller for the PV array system with a resistive load $R = 12\,\Omega$. Similarly, the output-voltage waveform is very close to a sine waveform. Figure 5 shows the output voltage of a PV array system controlled by the conservative SMC at a trigger angle, changing from no load to full load ($R = 12\,\Omega$). The figure shows that the transient voltage drop does not recover quickly and the controller is not able to compensate well. Figure 6 shows the output voltage of the PV array system using the proposed controller at trigger angle, changing from no load to full load

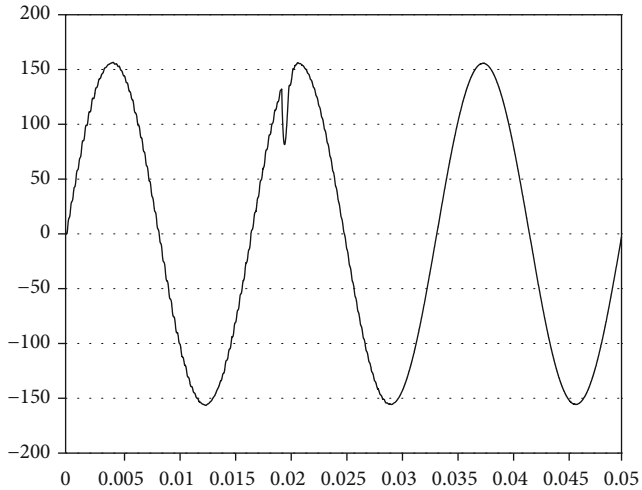

Figure 5: Output voltage of a PV array system for the conservative SMC under step load changing (vertical: 50 V/div; horizontal: 5 ms/div).

($R = 12\,\Omega$). The graph shows that the transient voltage drop is recovered within a very short period of time with excellent compensation capability. Figure 7 shows the output voltage of the PV array system under rectifier-type load with the conservative SMC. It can be seen that the output voltage is a distorted sine waveform with a high %THD value of 12.36%. Figure 8 shows the output waveform of the PV array system controlled by the proposed controller under rectified load. The output-voltage waveform is very close to the required sinusoidal reference voltage (low %THD value of 0.08%). It can be seen that the proposed PV array system has a better performance than the conservative sliding mode controlled PV array system. A comparison is listed in Table 1 of the voltage drops and THD values of the conservative SMC and the proposed controller for transient loading and steady-state loading. The proposed controller reveals small voltage drop

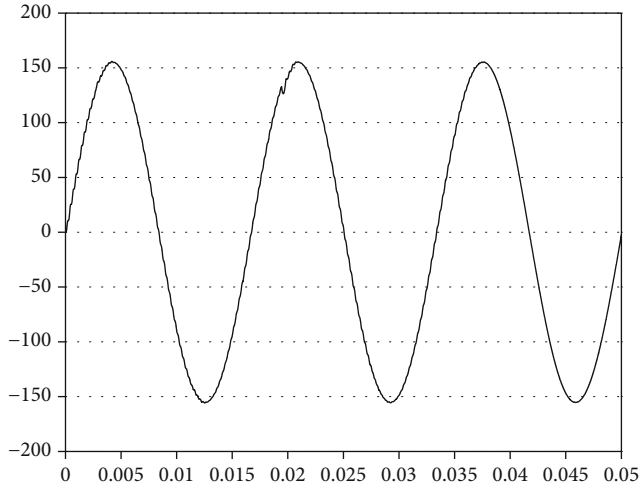

Figure 6: Output voltage of a PV array system for the proposed controller under step load changing (vertical: 50 V/div; horizontal: 5 ms/div).

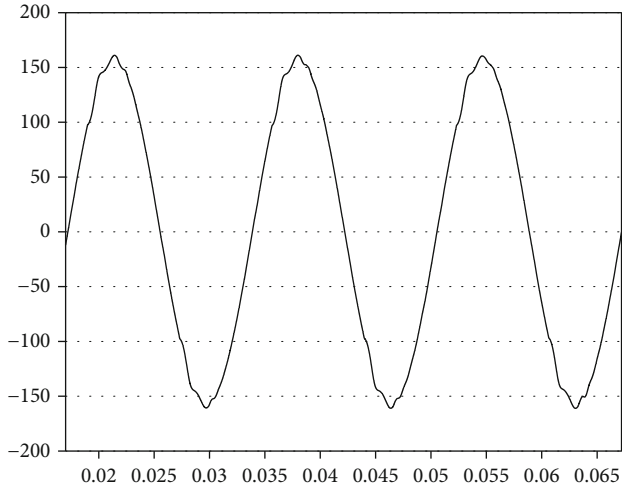

Figure 7: Output voltage of a PV array system for the conservative SMC under rectifier load (vertical: 50 V/div; horizontal: 5 ms/div).

and low THD values with the voltage waveforms close to the required sinusoidal reference voltages. However, in the case of rectified loads, the output voltage of the PV array system controlled by the conservative SMC has a distortion rate of more than 5%, while the proposed PV array system has a distortion rate of less than 5%, which is better than the 519 harmonic control standard set by the American Institute of Electrical and Electronics Engineers. The results are compared with existing work hereunder. A SMC is designed for active and reactive power control of the renewable energy generations, while the PSO algorithm allows optimizing the SMC parameters. The system can generate real power within 1% of the required power at a fast time, indicating stable power. Although the proposed method is capable of producing acceptable transience and steady-state actions, the speed of the system state driving to the sliding surface remains to be refined [49]. The single-phase inverter based on the SMC is

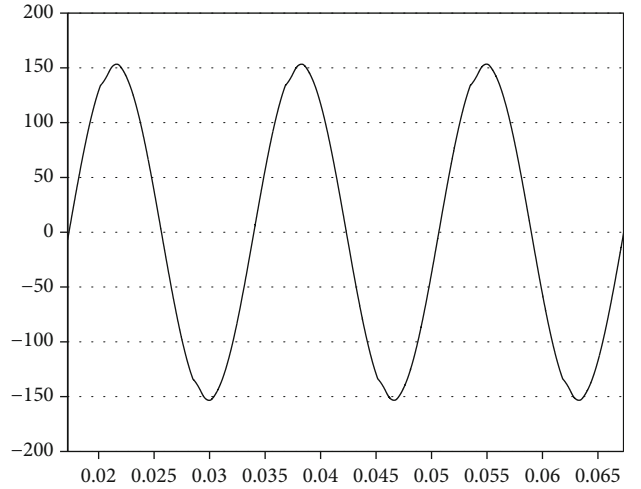

Figure 8: Output voltage of a PV array system for the proposed controller under rectifier load (vertical: 50 V/div; horizontal: 5 ms/div).

Table 1: Output voltage drop and %THD.

	Proposed controller	Conservative SMC
Step loads Voltage drop	$6.67V_{max}$	$51.3V_{max}$
Full resistive load %THD	0.02%	0.05%
Rectifier load %THD	0.08%	12.36%

connected to the grid with the purpose of establishing optimized PV delivery. Meanwhile, the overall circuit structure uses a boost converter with a PSO algorithm optimized fuzzy logic scheme, which yields the MPPT. The presented inverter provides quick dynamic response; nevertheless, the steady state should be investigated under severely nonlinear loading perturbations [50]. A double feedback controller realized by the SMC and proportional-integral control has been applied to the microsource inverter, where a PSO algorithm is employed for the optimization of the control parameters. The sliding-mode reaching law does not precisely strike the requisite sliding manifold, so the resulting waveforms still suffer from considerable distortion [51]. A brushless DC motor actuated water pumping system dependent on the PV supply has been proposed. This system offers several features such as no additional DC-DC converter hardware, sliding mode controller implementing sensorless speed controller, and hybrid whale optimization-perturbation and observation algorithm getting the maximum available power either in partially shaded and normally operating conditions. Because the applied technology fails to remove the chattering effect, there is a steady-state error around the state trajectory [52]. The passive-based control has been developed for grid-connected inverters. The PSO algorithm and Kalman filter observer give the simplification of the passive-based control parameters design and the diminution of sensors number, respectively. It has revealed an improvement in the total harmonic distortion and dynamic behavior both during steady state and transient loading; however, a little oscillation

in the output waveform appears due to the potential for premature convergence with conventional PSO [53]. In spite of the fact that the proposed system's performance does not greatly overtake the THD results from the latest reports, the proposed controller is unsophisticated, straightforward to comprehend, and quick to converge, thus affording better target tracking control. It can be a valuable referral for readers concerned with renewable energy converters as well as AIoT applications.

5. Conclusions

With the proposed controller, it is possible to employ a gradient particle swarm optimization algorithm to detect the global maximum power point of the photovoltaic array in the presence of partial shading while using the unique advantages of the finite-time terminal attractor to offer fast convergence of the system state under uncertain interferences, quiver, and reduction of steady-state errors for tracking control. The simulated operating conditions of the photovoltaic arrays, such as voltage, current, and power, are also stored, collated, monitored, and analysed by the IoT platform to enhance the reliability and integrity of the system. The controller developed in this manner can create the maximum power output from the solar panel and retain the highest energy conversion efficiency in the event of partial shading. The proposed controller has good steady-state and transient response behavior in terms of total harmonic distortion and momentary voltage drop under rectifier loading and step load varying conditions, displaying the waveforms are close to the required sinusoidal reference voltage. However, the output voltage of the conservative SMC of the PV array system suffers from higher than 5% THD and greater voltage drop for the same testing load conditions. As a result, the proposed PV array system actually yields promising performance when subjected to partial shading circumstances. This paper has innovative highlights which can be summarized as follows. (i) The proposed controller can be used not only for interleaved Boost DC–DC converter but also directly for Cuk, Sepic, and Zeta DC-DC converters, which provides the advantage of extended applications. (ii) The proposed controller incorporating AIoT allows the information analysis of the voltage, current, and power in the PV system, which will be the future trend of smart city development. (iii) The proposed controller is capable of yielding high-quality AC supply, which can be fully adopted in the future for various renewable energy sources, such as wind and hydrogen energies.

Conflicts of Interest

The authors declare that there is no conflict of interest regarding the publication of this article.

Acknowledgments

The authors gratefully acknowledge the financial support of the Ministry of Science and Technology of Taiwan, R.O.C., under project number MOST 110-2221-E-214-021.

References

[1] M. Saad and A. M. Eltamaly, *Advanced Technologies for Solar Photovoltaics Energy Systems*, Springer, Switzerland, 2021.

[2] A. J. Yaman and H. Eklas, *Photovoltaic Systems: Fundamentals and Applications*, Springer, Switzerland, 2022.

[3] M. Moh, K. P. Sharma, R. Agrawal, and V. G. Diaz, *Smart IoT for Research and Industry*, Springer, Switzerland, 2022.

[4] K. Vinod, K. B. Ranjan, J. Dheeraj, and B. Ramesh, *Power Electronics, Drives, and Advanced Applications*, CRC Press, Boca Raton, FL, USA, 2020.

[5] H. Yang, *Modeling and Control of Power Electronic Converters for Microgrid Applications*, Springer, Switzerland, 2022.

[6] F. L. Luo and H. Ye, *Power Electronics: Advanced Conversion Technologies*, CRC Press, Boca Raton, FL, USA, 2018.

[7] E.-C. Chang, "Applying robust intelligent algorithm and Internet of things to global maximum power point tracking of solar photovoltaic systems," *Wireless Communications and Mobile Computing*, vol. 2020, Article ID 8882482, 10 pages, 2020.

[8] A. R. Gautam, L. Umanand, and R. B. Subba, "Current control of boost converter for PV interface with momentum-based perturb and observe MPPT," *IEEE Transactions on Industry Applications*, vol. 57, no. 4, pp. 4071–4079, 2021.

[9] B. Shamik, S. K. P. Dattu, S. Susovon, and M. Sukumar, "Steady output and fast tracking MPPT (SOFT-MPPT) for P&O and InC algorithms," *IEEE Transactions on Sustainable Energy*, vol. 12, no. 1, pp. 293–302, 2021.

[10] P. Imran, S. Immad, M. Saad, S. Adil, T. Mohd, and A. Basem, "Most valuable player algorithm based maximum power point tracking for a partially shaded PV generation system," *IEEE Transactions on Sustainable Energy*, vol. 12, no. 4, pp. 1876–1890, 2021.

[11] B. Badreddine, A. Fahad, H. Noureddine, K. Sami, and S. M. Ghoneim, "Fractional-fuzzy PID control approach of photovoltaic-wire feeder system (PV-WFS): simulation and HIL-based experimental investigation," *IEEE Access*, vol. 9, pp. 159933–159954, 2021.

[12] V. I. Utkin, "Variable structure systems with sliding modes," *IEEE Transactions on Automatic Control*, vol. 22, no. 2, pp. 212–222, 1977.

[13] M. Axaykumar and B. Bijnan, *Emerging Trends in Sliding Mode Control: Theory and Application*, Springer, Singapore, 2021.

[14] U. Itkis, *Control Systems of Variable Structure*, Wiley, New York, 1976.

[15] C. Y. Chan, "Servo-systems with discrete-variable structure control," *Systems Control Letters*, vol. 17, no. 4, pp. 321–325, 1991.

[16] H. Sira-Ramirez, "Sliding regimes in general non-linear systems: a relative degree approach," *International Journal of Control*, vol. 50, no. 4, pp. 1487–1506, 1988.

[17] Z. Doulgeri, "Sliding regime of a nonlinear robust controller for robot manipulators," *IEE Proceedings-Control Theory and Applications*, vol. 146, no. 6, pp. 493–498, 1999.

[18] G. Bartolini, L. Fridman, A. Pisano, and E. Usai, *Modern Sliding Mode Control Theory*, Springer-Verlag, Berlin, 2008.

[19] R. Chinnappan, P. Logamani, and R. Ramasubbu, "Fixed frequency integral sliding-mode current-controlled MPPT boost converter for two-stage PV generation system," *IET Circuits, Devices & Systems*, vol. 13, no. 6, pp. 793–805, 2019.

[20] B. Banerjee and W. W. Weaver, "Generalized geometric control manifolds of power converters in a DC microgrid," *IEEE Transactions on Energy Conversion*, vol. 29, no. 4, pp. 904–912, 2014.

[21] H. F. Feshara, A. M. Ibrahim, N. H. El-Amary, and S. M. Sharaf, "Performance evaluation of variable structure controller based on sliding mode technique for a grid-connected solar network," *IEEE Access*, vol. 7, pp. 84349–84359, 2019.

[22] M. Alsumiri, "Residual incremental conductance based nonparametric MPPT control for solar photovoltaic energy conversion system," *IEEE Access*, vol. 7, pp. 87901–87906, 2019.

[23] P. Peltoniemi, P. Nuutinen, and J. Pyrhonen, "Observer-based output voltage control for DC power distribution purposes," *IEEE transactions on power electronics*, vol. 28, no. 4, pp. 1914–1926, 2013.

[24] X. B. Wu, Q. Liu, M. L. Zhao, and M. Y. Chen, "Monolithic quasi-sliding-mode controller for SIDO buck converter with a self-adaptive free-wheeling current level," *Journal of Semiconductors*, vol. 34, no. 1, 2013.

[25] L. Shen, D. D. Lu, and C. Li, "Adaptive sliding mode control method for DC–DC converters," *IET Power Electronics*, vol. 8, no. 9, pp. 1723–1732, 2015.

[26] X. D. Du, X. Fang, and F. Liu, "Continuous full-order nonsingular terminal sliding mode control for systems with matched and mismatched disturbances," *IEEE Access*, vol. 7, pp. 130970–130976, 2019.

[27] V. C. Nguyen, A. T. Vo, and H. J. Kang, "A finite-time fault-tolerant control using non-singular fast terminal sliding mode control and third-order sliding mode observer for robotic manipulators," *IEEE Access*, vol. 9, pp. 31225–31235, 2021.

[28] H. Z. Hou, X. H. Yu, L. Xu, R. Kamal, and Z. W. Cao, "Finite-time continuous terminal sliding mode control of servo motor systems," *IEEE Transactions on Industrial Electronics*, vol. 67, no. 7, pp. 5647–5656, 2020.

[29] P. D. Ge, Y. Zhu, C. G. Tim, and F. Teng, "Resilient secondary voltage control of islanded microgrids: an ESKBF-based distributed fast terminal sliding mode control approach," *IEEE Transactions on Power Systems*, vol. 36, no. 2, pp. 1059–1070, 2021.

[30] S. K. Cherukuri and S. R. Rayapudi, "Enhanced grey wolf optimizer based MPPT algorithm of PV system under partial shaded condition," *International Journal of Renewable Energy Development*, vol. 6, no. 3, pp. 203–212, 2017.

[31] A. Yahiaoui, F. Fodhil, K. Benmansour, M. Tadjine, and N. Cheggaga, "Grey wolf optimizer for optimal design of hybrid renewable energy system PV- diesel generator-battery: application to the case of Djanet city of Algeria," *Solar Energy*, vol. 158, pp. 941–951, 2017.

[32] N. Zhao, C. Roberts, and S. Hillmansen, "The application of an enhanced brute force algorithm to minimise energy costs and train delays for differing railway train control systems," *Proceedings of the Institution of Mechanical Engineers Part F Journal of Rail and Rapid Transit*, vol. 2288, no. 2, pp. 158–168, 2014.

[33] Y. Y. Jia, J. Q. Wang, and Q. Y. Xiao, "Multiple groups of gradient particle swarm optimization and its application in optimal operation of reservoir," in *Proceedings of the 2014 10th International Conference on Natural Computation (ICNC)*, pp. 622–626, Xiamen, China, 2014.

[34] B. T. Zhang and R. Yahya, "Including design sensitivity into particle swarm optimization: adaptive gradient-based techniques," in *Proceedings of the 2015 Asia-Pacific Microwave Conference (APMC)*, pp. 1–3, Nanjing, China, 2015.

[35] T. A. Loau, C. P. Jagdish, and S. Alex, "Solving economic dispatch problem under valve- point loading effects and generation constrains using a multi-gradient PSO algorithm," in *Proceedings of the 2018 International Joint Conference on Neural Networks (IJCNN)*, pp. 1–8, Rio de Janeiro, Brazil, 2018.

[36] N. Subhrapratim, S. Aditya, S. Ritankar, B. Suharta, K. S. Jamuna, and K. S. Subir, "Minimizing wirelength with bend reduction using gradient descent PSO hybrid in VLSI global routing," in *Proceedings of the 2021 Devices for Integrated Circuit (DevIC)*, pp. 401–405, Kalyani, India, 2021.

[37] D. L. Cavalca and A. S. Fernandes, "Gradient-based mechanism for PSO algorithm: a comparative study on numerical benchmarks," in *Proceedings of the 2018 IEEE Congress on Evolutionary Computation (CEC)*, pp. 1–7, Rio de Janeiro, Brazil, 2018.

[38] U. Bartlomiej, K. Arkadiusz, and M. G. Lech, "Particle swarm optimization of the multioscillatory LQR for a three-phase four-wire voltage-source inverter with an *LC* output filter," *IEEE Transactions on Industrial Electronics*, vol. 62, no. 1, pp. 484–493, 2015.

[39] V. Mummadi and R. S. Anmol, "Iptimized power stage design of low source current ripple fourth-order boost DC–DC converter: a PSO approach," *IEEE Transactions on Industrial Electronics*, vol. 62, no. 3, pp. 1491–1502, 2015.

[40] K. E. Parsopoulos and M. N. Vrahatis, *Particle Swarm Optimization and Intelligence: Advances and Applications*, Information Science Reference, Hershey, PA, USA, 2010.

[41] K. Mohammad, T. Shamsodin, A. Cretu, H. Seyedkazem, and P. Edris, "PSO-based modeling and analysis of electrical characteristics of photovoltaic module under nonuniform snow patterns," *IEEE Access*, vol. 8, pp. 197484–197498, 2020.

[42] H. C. Shi, H. Q. Wen, Y. H. Hu, and L. Jiang, "Reactive power minimization in bidirectional DC–DC converters using a unified-phasor-based particle swarm optimization," *IEEE Transactions on Power Electronics*, vol. 33, no. 12, pp. 10990–11006, 2018.

[43] Y. W. Tzou and S. L. Jung, "Full control of a PWM DC-AC converter for AC voltage regulation," *IEEE Transactions on Aerospace and Electronic Systems*, vol. 34, no. 4, pp. 1218–1226, 1998.

[44] H. S. Kim and S. K. Sul, "A novel filter design for output LC filters of PWM inverters," *Journal of Power Electronics*, vol. 11, no. 1, pp. 74–81, 2011.

[45] M. Blachuta, B. Robert, and G. Rafal, "Sampling rate and performance of DC/AC inverters with digital PID control—a case study," *Energies*, vol. 14, no. 16, pp. 5170–5222, 2021.

[46] M. M. Noel and T. C. Jannett, "Simulation of a new hybrid particle swarm optimization algorithm," in *Proceedings of the 36th Southeastern Symposium on System Theory (SSST04)*, pp. 150–153, Atlanta, GA, USA, 2004.

[47] M. M. Noel, "A new gradient based particle swarm optimization algorithm for accurate computation of global minimum," *Applied Soft Computing*, vol. 12, no. 1, pp. 353–359, 2012.

[48] G. Cao, M. K. Lai, and A. Fakhrul, "Enhanced particle swarm optimisation algorithms for multiple-input multiple-output system modelling using convolved Gaussian process models," *International Journal of Intelligent Systems Technologies and Applications*, vol. 17, no. 3, pp. 1–17, 2018.

[49] S. Yousaf, A. Mughees, M. G. Khan, A. A. Amin, and M. Adnan, "A comparative analysis of various controller techniques for optimal control of smart nano-grid using GA and PSO algorithms," *IEEE Access*, vol. 8, pp. 205696–205711, 2020.

[50] A. Borni, A. Bouchakour, L. Zaghba, A. Thameur, A. Lakhdari, and N. Bessous, "Optimization of the fuzzy MPPT controller by PSO for the single-phase grid-connected photovoltaic system controlled by sliding mode," in *Proceedings of the 2018 6th International Renewable and Sustainable Energy Conference (IRSEC)*, pp. 1–7, Rabat, Morocco, 2018.

[51] J. Bian, C. Z. Zang, X. H. Li, B. Hu, and J. Liu, "The rapid development of three-phase grid-forming micro-source inverter based on SMC and PI control," in *Proceedings of the 2017 China International Electrical and Energy Conference (CIEEC)*, pp. 1–6, Beijing, China, 2017.

[52] S. G. Malla, P. Malla, J. M. R. Malla et al., "Whale optimization algorithm for PV based water pumping system driven by BLDC motor using sliding mode controller," *IEEE Journal of Emerging and Selected Topics in Power Electronics*, pp. 1–12, 2022.

[53] F. B. Zheng, W. M. Wu, B. L. Chen, and E. Koutroulis, "An optimized parameter design method for passivity-based control in a LCL-filtered grid-connected inverter," *IEEE Access*, vol. 8, pp. 189878–189890, 2020.